Int J Thermophys (2008) 29:2015–2024
DOI 10.1007/s10765-008-0538-2

Structure and Thermophysical Properties of Molten BaGe Using Electrostatic Levitation Technique

Akiko Ishikura · Akitoshi Mizuno · Masahito Watanabe · Tadahiko Masaki · Takehiko Ishikawa · Shinichi Yoda

Published online: 27 November 2008

Abstract BaGe alloys with two compositions near their eutectic point form open framework structures called the clathrate structure. These BaGe compounds with the clathrate structure can be made by rapid solidification from their liquid state. However, the formation mechanism of the clathrate structure has not been clarified due to lack of information on their liquid-state structure and properties. Since BaGe alloy melts have very high reactivity, it is difficult to measure the thermophysical properties of them by ordinary methods using a container. Therefore, a containerless technique must be used to measure the thermophysical properties of BaGe melts. Using the electrostatic levitation (ESL) technique as a containerless technique, the thermophysical properties (density, surface tension, and viscosity) of BaGe melts around the eutectic composition were measured in order to clarify the formation mechanism of the clathrate structure, and also the structure of them was observed by using the high-energy X-ray diffraction method combined with ESL. From experimental results, it was observed that the short-range order based on the clathrate structure exists even in the liquid state at the clathrate-forming compositions.

Keywords BaGe compound · Clathrate · Density · Electrostatic levitation · Surface tension · Viscosity

A. Ishikura · A. Mizuno · M. Watanabe (✉)
Department of Physics, Gakushuin University,
1-5-1 Mejiro, Tokyo 171-8588, Japan
e-mail: masahito.watanabe@gakushuin.ac.jp

T. Masaki · T. Ishikawa · S. Yoda
Japan Aerospace Exploration Agency (JAXA),
1-1-1 Sengen, Tsukuba 305-8505, Japan

1 Introduction

BaGe alloys with two compositions, Ba_8Ge_{43} [1] and Ba_6Ge_{25} [2], near their eutectic point [3] form an open framework structure, which is identified as a clathrate compound from its similarity to the clathrate structure of a gas hydrate. Gas hydrates have a structure in which water molecules are linked by hydrogen bonds to form a three-dimensional network with cage structure trapped gas molecules, CO_2, Ar, and methane, etc., inside the cages [4]. In the clathrate compounds, the group-IV elements (framework atoms) form a three-dimensional network with a cage structure in which the group-II elements (guest atoms) are ionically bound. The framework atoms form covalent bonds with a slightly distorted tetrahedral coordination environment [5]. From these characteristic structures, clathrate compounds have lower thermal conductivities, in which this property and its temperature dependence show features of the thermal conductivity of glass materials, rather than compounds with a diamond structure. This glass-like low thermal conductivity is due to the strong scattering of heat-carrying acoustic phonons by the rattling motions of the guest atoms in the cages [6]. On the other hand, from electron density analysis and band-structure calculations, these clathrate compounds are semiconductors. Therefore, the glass-like thermal conductivities and the electrical conductivities of semiconductors make clathrate compounds promising thermoelectric materials for solid-state cooling and power generation devices [7].

Some clathrate compounds are unstable in a moisture environment. Thus, if we explore new materials for thermoelectrics in clathrate compounds, they must be stable in air and a moisture environment. The clathrate compounds based on Ge atoms are stable in air and a moisture atmosphere, and $Ba_8Ga_{16}Ge_{30}$ [8] shows high values of the thermoelectric figure of merit $ZT = S^2\sigma/(\kappa T)$, where T is the temperature, S is the Seebeck coefficient, σ is the electrical conductivity, and κ is the thermal conductivity. These clathrate compounds based on the Ge atoms can be synthesized by direct fusion from pure elements. Since clathrate phases are unstable phases, rapid solidification, which is not characterized by a high cooling rate such as that of amorphous metals, from their liquid state is necessary. However, the formation mechanism of clathrate structure from its liquid state has not been clarified because of the lack of information on the liquid-state structure and properties.

Since BaGe melts have very high reactivity, it is difficult to measure their thermophysical properties by ordinary methods using a container. Therefore, we must use a containerless technique to measure the thermophysical properties of BaGe melts. Using electrostatic levitation (ESL) as a containerless technique [9,10], the thermophysical properties (density, surface tension, and viscosity) of BaGe melts near the eutectic composition were measured in order to clarify the formation mechanism of the clathrate structure. Since the BaGe clathrate compounds are obtained from their liquid state by rapid solidification, we expect that the basic atomic arrangement (short-range order) of the clathrate structure would be formed even in the liquid state. If these atomic arrangements, as the basis of clathrate structures, exist in the liquid state, the thermophysical properties would also show characteristic phenomena at the composition associated with the clathrate structure. We found that from experimental results of thermophysical property measurements and structural analysis of liquid states by

using the high-energy X-ray diffraction method combined with ESL, the short-range order based on the clathrate structure exists even in the liquid state at clathrate-forming compositions.

2 Experimental

2.1 Preparation of BaGe Samples

For measurements of the density, surface tension, and viscosity of BaGe melts, we initially prepared solid samples of BaGe compounds with a spherical shape by a laser heating method using a CO_2 laser (wavelength of 10.5 μm) with a custom-designed vacuum furnace. Ba atoms have very high reactivity for oxygen, so we prepared a mixture of high-purity (5N up) Ba and Ge at the desired mole ratio in a vacuum furnace under an Ar atmosphere using a glove box. Especially for Ba_8Ge_{43} and Ba_6Ge_{25} of clathrate-forming compositions, we confirmed that the solid samples have a clathrate structure by x-ray powder diffraction using Cu $K-\alpha$ radiation with Rietveld refinements using RITAN 2000 [11]. Compositions of clathrate compounds were determined by using scanning electron microscopy (SEM) with an electron probe micro-analyzer (EPMA). These solid samples are stable under atmospheric conditions, so we easily transfer them to the ESL furnace.

2.2 Electrostatic Levitation System

The ESL system [10] used in the present studies is shown in Fig. 1. It consisted of a vacuum chamber that was evacuated to 10^{-5} Pa before processing [12,13]. The chamber housed ESL electrodes that allowed a sample charged by electronic emission

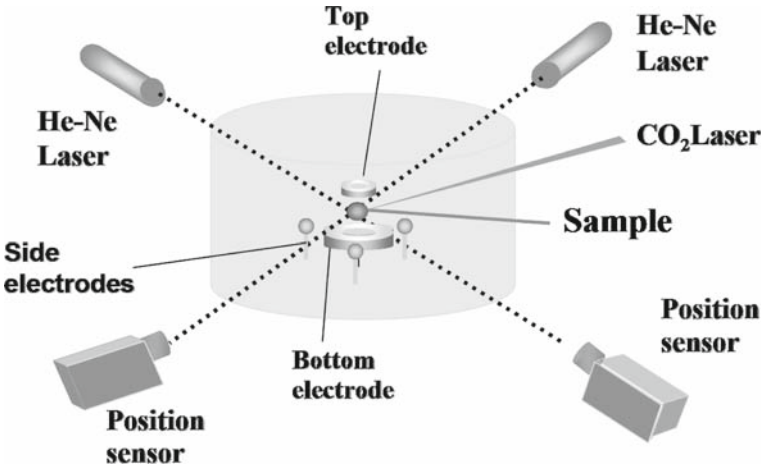

Fig. 1 Experimental setup of the electrostatic levitation system for measurement of thermophysical properties of BaGe melts

to maintain a fixed position by a feedback loop. Two disk electrodes were used for vertical control, and four spherical electrodes were utilized for horizontal control. The positioning control relied on two sets of orthogonally disposed He–Ne lasers and the associated position sensors. The sample position information measured by the sensors was fed to a computer that inputs new values of x, y, and z to high-voltage amplifiers so that a prefixed position could be maintained. For heating, a CO_2 laser (wavelength of 10.5 μm) beam was used to directly irradiate the sample, because BaGe compounds do not have such high-melting temperatures. This configuration, together with precise laser power control (0 W to 200 W), provided position stability and allowed control of the sample rotation. The temperature of the samples was observed by two pyrometers operating at 900 nm and 960 nm (120 Hz acquisition rate) with a temperature range from 1,070 K to 3,800 K. The temperature was calibrated to the true temperature using the melting plateau of the material. The sample was observed by three charged-coupled device cameras. One camera that monitored both the electrode assembly and the sample was observed by two cameras, located at 90° of each other, in conjunction with a background light, and provided a magnified view of the sample.

2.3 Procedure of Measurements of Density, Surface Tension, and Viscosity

BaGe compounds samples were electrostatically levitated by applying a 7.5 kV voltage between the main electrodes. To improve the sample stability and to minimize the time required to reach the molten phase, the laser beams were oriented in such a way to induce a slight equatorial rotation ($\ll$5 Hz), thus preventing any polar rotation. Once the sample was spin-stabilized, the laser beams were realigned in such a way to produce no torque on the sample to avoid an increase in the rotational rate which could lead to bifurcation. The surface tension and viscosity of the BaGe melt were determined from the surface oscillations of the levitated droplet from its equilibrium shape [14]. The deviation of the droplet radius from a true sphere is described using the spherical harmonic function $Y_m^l(\theta, \varphi)$ by the equation,

$$r = R + \varepsilon Y_l^m(\theta, \varphi) = R + \varepsilon P_l^m(\theta)\cos(m\varphi)\cos(\omega_{l,m}t) \tag{1}$$

where R is the radius of a true sphere, ε is the amplitude of oscillation, ω is the frequency of the surface oscillations, $P_n(\cos(\theta))$ represents Legendre polynominals, and l and m are labels that indicate types of oscillations. For measurements of the surface tension and viscosity at the selected temperature, the $(l, m) = (2, 0)$ mode of the surface oscillations in the BaGe melt was generated by applying a small sinusoidal electric field on the levitation field. The surface oscillation frequency and the decay time of oscillation following the termination of the excitation field were detected and analyzed. Using the surface oscillation frequency ω after correcting for the non-uniform surface charge distribution [14], the surface tension σ can be obtained from

$$\omega^2 = \frac{8\sigma}{\rho r^3} Y \tag{2}$$

where r is the radius of the sample, ρ is the density, and Y is a correction factor depending on the drop charge [14], the permittivity of vacuum, and the applied electric field. Similarly, using the decay time τ given by the same signal, the viscosity η was obtained from

$$\eta = \frac{\rho r^2}{5\tau} \tag{3}$$

In Eqs. 2 and 3, real-time values of the radius and density data were used to prevent any distortion in the measured properties due to sample evaporation. The uncertainty of the measurements was estimated to be better than 20 % from the response of the oscillation detector and from the density measurements.

3 Results and Discussion

3.1 Density

Density measurements of the BaGe melt were obtained over a temperature range from 1,100 K to 1,600 K and extended into the undercooled region by nearly 100 K as shown in Fig. 2. Ba_8Ge_{43} (Ba 15.7 at%) and Ba_6Ge_{25} (Ba 19.4 at%) are clathrate-forming compositions. The density exhibited a linear behavior as a function of temperature and can be fitted by the relationship,

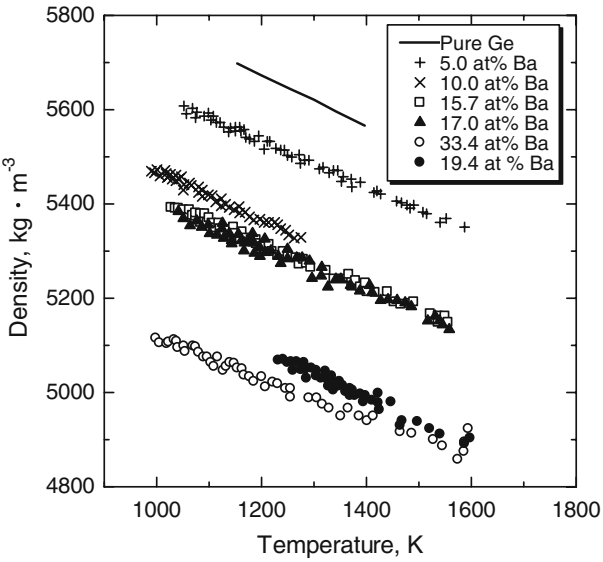

Fig. 2 Temperature dependence of the density of BaGe melts for each composition near their eutectic composition

$$\rho(T) = \rho_{\mathrm{l}} + \rho_T (T - T_{\mathrm{l}}) \tag{4}$$

where T_{l} is the eutectic temperature, ρ_{l} is the density at the eutectic temperature, and ρ_T is the temperature coefficient of density in the range from 1,100 K to 1,600 K. The values for each composition are summarized in Table 1. These density measurements are the first to cover a wide compositional range. From these results, we cannot recognize the feature of clathrate-forming compositions in the density, so we plotted the constant temperature molar volume at 1,100 K as shown in Fig. 3. In this figure the straight line shows the estimated molar volume from the simple sum relationship between the molar concentration and the molar volume;

$$V_{\mathrm{total}}(T) = C_{\mathrm{Ba}} V_{\mathrm{Ba}}(T) + (1 - C_{\mathrm{Ba}}) V_{\mathrm{Ge}}(T) = \frac{\rho(T)}{C_{\mathrm{Ba}} M_{\mathrm{Ba}} + (1 - C_{\mathrm{Ba}}) M_{\mathrm{Ge}}} \tag{5}$$

where V_{total} is the total molar volume of the BaGe melt, C_{Ba} is the molar concentration of Ba, V_{Ba} and V_{Ge} are the molar volumes of Ba and Ge, and M_{Ba} and M_{Ge} are the molar masses of Ba and Ge. From this figure, we recognize that the molar volume of the Ba_6Ge_{25} melt, which is the composition of a clathrate-forming compound, was determined using a linear relationship of the simple sum rule. We expect from this result that, at the clathrate-forming compositions, the atomic arrangement in the short range would be different from other compositions. This difference of the molar volume dependence on mole fraction will be discussed again along with the viscosity data.

3.2 Surface Tension

The surface-tension measurements of BaGe melts were also obtained over a temperature range from 1,100 K to 1,600 K and extended into the undercooled region by nearly 100 K as shown in Fig. 4. The surface tension exhibited a linear behavior as a function of temperature and can be fitted by the relationship,

Table 1 Density parameters, ρ_{l} and ρ_T, in Eq. 4 for BaGe melts

	T_{l} (K)	ρ_{l} (kg · m^{-3})	ρ_T (kg · m^3 · K^{-1})
Ge	1,211 (Melting temperature)	5,828	−0.542
5.0 at% Ba	1,083	5,591	−0.486
10.0 at% Ba	1,083	5,590	−0.524
15.7 at% Ba	1,083	5,372	−0.472
17.0 at% Ba	1,083	5,361	−0.463
19.4 at% Ba	1,088	5,082	−0.427
33.3 at% Ba	1,343	5,021	−0.499

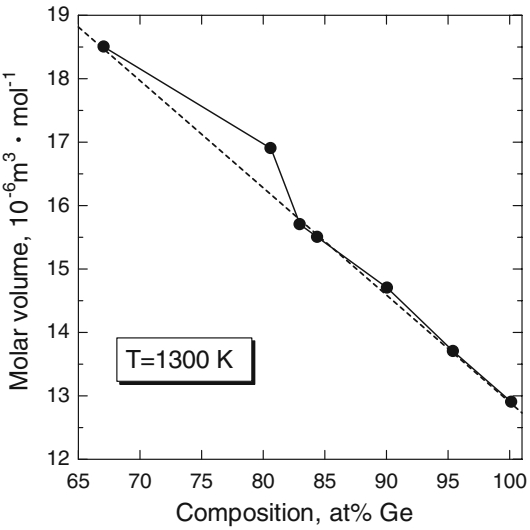

Fig. 3 Molar volume of BaGe melts for each composition at 1,300 K. Straight line shows a simple sum relation of molar volumes for each composition

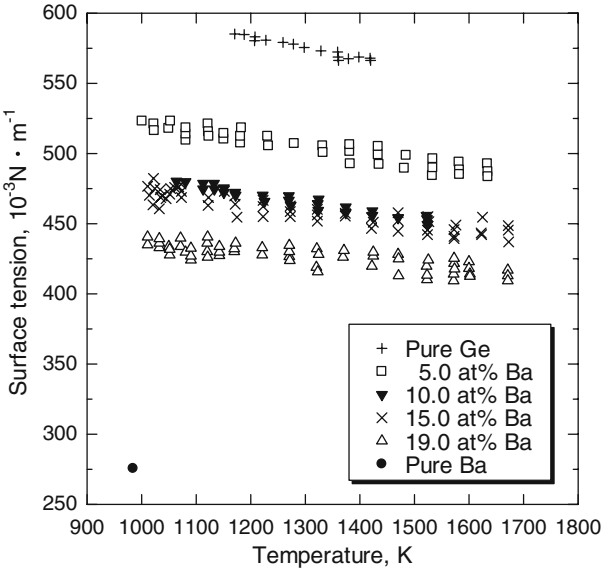

Fig. 4 Temperature dependence of the surface tension of BaGe melts for each composition

$$\sigma(T) = \sigma_1 + \sigma_T(T - T_1) \tag{6}$$

where σ_1 is the surface tension at the eutectic temperature, and σ_T is the temperature coefficient of the surface tension in the range from 1,100 K to 1,600 K. These measurements are also the first to cover the compositional dependence. From these results, the temperature dependence of the surface tension of each composition is almost the same as for the pure Ge melt [15], and no differences in clathrate-forming

Table 2 Surface-tension parameters, σ_1 and σ_T, in Eq. 6 for BaGe melts

	T_1 (K)	σ_1 $(10^{-3}\mathrm{N}\cdot\mathrm{m}^{-1})$	σ_T $(10^{-3}\mathrm{N}\cdot\mathrm{m}^{-1}\cdot\mathrm{K}^{-1})$
Ge	1,211 (Melting temperature)	582.8	−0.07772
5.0 at% Ba	1,083	517.4	−0.05291
10.0 at% Ba	1,083	477.0	−0.05869
15.7 at% Ba	1,083	469.6	−0.04830
19.4 at% Ba	1,088	435.2	−0.03197

compositions were observed. This means that the surface tension of BaGe melts in this composition range is dominated by Ge. For the case of a binary element system, the surface tension is dependent on the excess Gibbs energy in the surface due to the atomic surface structure [16] (Table 2).

3.3 Viscosity

We obtained the viscosity of the BaGe melts from the decay time of surface oscillation damping of levitated droplets over the same temperature range as the density and surface-tension measurements including about 100 K undercooling. Figure 5 shows the viscosity data as a function of temperature. From this result, it is observed that the temperature dependence of the viscosity can be classified into two groups according to the composition range. These groups correspond to the clathrate structure-forming

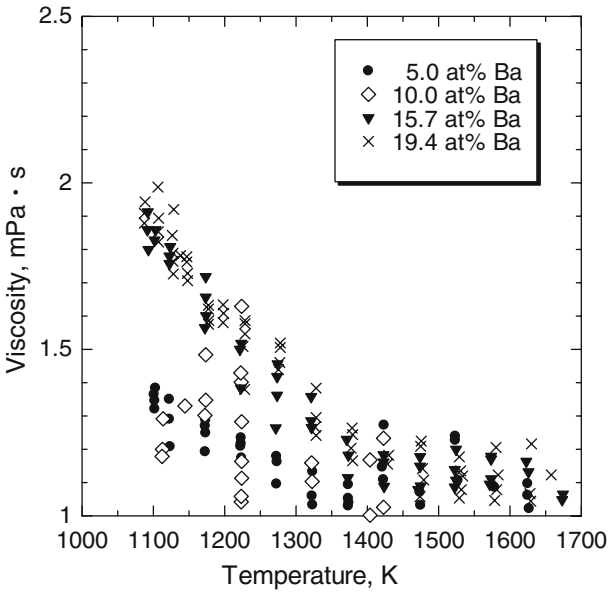

Fig. 5 Temperature dependence of the viscosity of BaGe melts for each composition

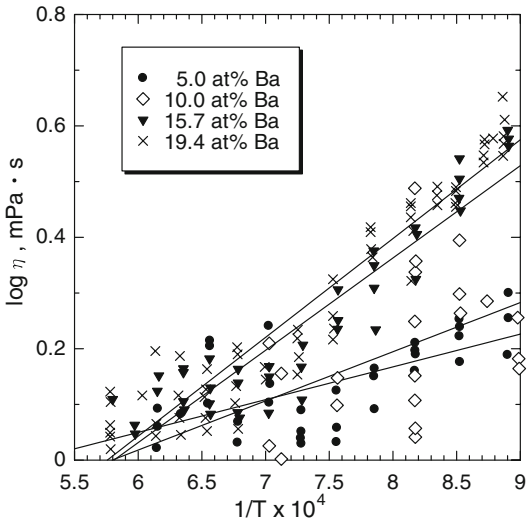

Fig. 6 Logarithmic plot of the viscosity of BaGe melts versus inverse temperature

compositions and the non-clathrate structure-forming compositions. For both groups of viscosity data, we find that they can be fitted by the Arrhenius form $\eta(T) = \eta_0 \exp(\frac{E}{RT})$, where R is the universal gas constant (8.3144 J $\cdot$ mol^{-1} $\cdot$ K^{-1}), E is the activation energy corresponding to the viscous flow, and η_0 is the pre-exponential viscosity.

In Fig. 6, we plotted the viscosities at each composition on a logarithmic scale versus the inverse temperature. From this figure, we can see that the viscosities for each composition can be fitted with a linear relationship. From the present experimental results, we understand that the clathrate-forming compositions have a larger activation energy compared to that of the non-clathrate-forming compositions. The high-activation energy of viscous flow means that atoms in the liquid state cannot be easily moved, so it is considered that for the clathrate-forming composition, atoms in the liquid state form an ordered structure. This means that for the clathrate-forming compositions, the atomic arrangement at short range would be a tightly formed cage structure similar to the clathrate structure.

In Fig. 3, the molar volume is also different for the clathrate-forming compositions compared to the non-clathrate-forming compositions. Both viscosity and molar volume changes at the clathrate-forming compositions are consistent with the ordered structure in liquid states. This ordered structure would be the pre-structure of the clathrate structure. If the pre-structure of the clathrate structure would be formed in a BaGe melt at a clathrate-forming composition, the cage-like structure of short-range order would exist in the liquid state. To form the cage-like structure of short-range order in the liquid state, atoms show crystalline bonding and thus the liquid with the cage-like atomic arrangements of short-range order have a larger volume than that of the liquid with the close-packed arrangement at short range. Therefore, the differences of molar volume and viscosity at clathrate-forming compositions would be attributed to the formation of the pre-structure of the clathrate structure. We confirmed the cage-like

structure of short-range order in BaGe melts at clathrate-forming compositions using an energy X-ray diffraction method combined with ESL using synchrotron radiation of BL04B2 at SPring-8, Japan. Details of the structure analysis experiments were described elsewhere [17].

4 Conclusion

The thermophysical properties, density, surface tension, and viscosity, of BaGe melts near the eutectic composition were precisely measured for the first time. We also succeeded in measuring the temperature dependence of these thermophysical properties over a wide compositional range. The viscosity at clathrate-forming compositions shows a different temperature dependence from that at other compositions, and also the density at clathrate-forming compositions shows a different temperature dependence than that at other compositions. We expect from these thermophysical property measurements that the cage-like short-range order based on the clathrate structure would exist even in the liquid state at the clathrate-forming compositions.

Acknowledgments This work was supported by the "Ground-based Research Program for Space Utilization" promoted by the Japan Space Forum and also supported by the Grant-in-Aid for Scientific Research (KAKENHI No. 19560747).

References

1. W. Carrillo-Cabrera, J. Curda, K. Peters, S. Paschen, M. Baenitz, Y. Grin, H.G. von Schenering, Z. Kristallogr.-New Cryst. Struct. **215**, 321 (2000)
2. W. Carrillo-Cabrera, J. Curda, H.G. von Schnering, S. Paschen, Y. Grin, Z. Kristallogr.-New Cryst. Struct. **215**, 207 (2000)
3. W. Carrillo-Cabrera, H. Borrmann, S. Paschen, M. Baenitz, F. Steglich, Y. Grin, J. Solid State Chem. **178**, 715 (2005)
4. G.A. Jeffrey, in *Inclusion Compounds*, vol. 1, ed. by J.L. Atwood, J.E.D. Davis, D.D. MacNicol (Academic Press, London, 1984), p. 135
5. J.S. Kasper, P. Hagenmuller, M. Pouchard, C. Cros, Science **150**, 1713 (1965)
6. J.L. Cohn, G.S. Nolas, V. Fessatisdis, T.H. Metcalf, G.A. Slack, Phys. Rev. Lett. **82**, 779 (1999)
7. G.S. Nolas, J.L. Cohn, G.A. Slack, S.B. Schujman, Appl. Phys. Lett. **73**, 178 (1998)
8. B.C. Sales, B.C. Chakoumakos, R. Jin, J.R. Thompson, D. Mandrus, Phys. Rev. **B63**, 245113 (2001)
9. W.-K. Rhim, S.K. Chung, D. Barber, K.F. Man, G. Gutt, A. Rulison, R.E. Spjut, Rev. Sci. Instrum. **64**, 2961 (1993)
10. T. Ishikawa, P.-F. Paradis, S. Yoda, Rev. Sci. Instrum. **72**, 2490 (2001)
11. F. Izumi, T. Ikeda, Mater. Sci. Forum **321–324**, 198 (2000)
12. S.K. Chung, D.B. Thiessen, W.-K. Rhim, Rev. Sci. Instrum. **67**, 3175 (1996)
13. W.-K. Rhim, K. Ohsaka, P.-F. Paradis, Rev. Sci. Instrum. **70**, 2796 (1999)
14. T. Ishikawa, P.-F. Paradis, T. Itami, S. Yoda, Meas. Sci. Technol. **16**, 443 (2005)
15. W.-K. Rhim, T. Ishikawa, Int. J. Thermophys. **21**, 429 (2000)
16. T. Tanaka, MRS Bull. **24**, 45 (1999)
17. A. Ishikura, A. Mizuno, M. Watanabe, T. Masaki, T. Ishikawa, S. Kohara, J. Am. Ceram. Soc. **90**, 738 (2007)